Stratus Surge Prediction along the Central California Coast

PETER FELSCH

National Weather Service, Weather Service Office, Santa Maria, California

WOODROW WHITLATCH

Pacific Gas and Electric, San Francisco, California

(Manuscript received 8 May 1991, in final form 5 February 1993)

ABSTRACT

A simple decision-tree forecast scheme to predict the south–north development or movement of stratus along the central California coast is developed and tested. Known as "stratus surges," these mesoscale events are infrequently observed along the west coast of North America during the summer season. A subjective test involving inspection of visible image satellite photographs is successful in determining when the potential for surge development exists. Objective tests based on Oakland, California, radiosonde data and alongshore pressure gradients at 0000 UTC are developed to make "surge" and "no surge" forecasts for potential events. Skill scores show that forecasts based on the objective tests achieved a moderate level of accuracy. This technique is easy to apply and could serve as a basis for the development of other stratus surge forecast schemes along the coast.

1. Introduction

During the summer, the central California coast commonly experiences fair skies in the afternoon followed by the overnight development of stratus due to advection or in situ processes, which are triggered by very subtle changes in synoptic and/or mesoscale forces. A particularly difficult problem for the local forecaster is the prediction of the onset of stratus after one or more days of offshore flow and clear skies. One example is a unique type of onset known as a "stratus surge" that occurs when a narrow (mesoscale) band of marine stratus progresses northward along the coastline. A visible satellite image sequence showing the life cycle of a well-developed stratus surge along the central California coast is presented in Fig. 1. Figure 1a shows the initial development or stage for the potential northward surge of the stratus clouds. Figures 1b and 1c show the overnight progression of the stratus surge, which continues to progress northward during the day after the initial surge. Stratus surge events, considered anomalies because summer season coastal winds are predominantly northwesterly, act as mesoscale weather fronts as they progress along the coast. Their passage is marked by rising surface pressures, shifting winds, falling temperatures, and abrupt changes in ceilings and visibilities.

Corresponding author address: Dr. Peter Felsch, Weather Service Office, National Weather Service, Santa Maria Public Airport, Santa Maria, CA 93455.

The formation and movement of a stratus surge along the California coast can be a hazard to both aviation and marine interests, due to abrupt changes in ceiling heights, visibility, and wind shifts. Public, marine, and aviation forecasters face the problem of forecasting when the stratus surge will occur, as well as how long it will last along the coast. Very little documentation has been made of the synoptic and mesoscale characteristics associated with stratus surges along the West Coast. Forecasters, without the background knowledge of what synoptic and mesoscale characteristics to look for, find it difficult to forecast the initial onset of a stratus surge.

This study presents a climatology of stratus surge events and a forecast technique to predict events initiated along the central California coast. A brief review of past stratus surge studies along the West Coast of the United States is discussed in section 2. The climatological study and a conceptual model are documented in section 3. The forecast scheme is developed and tested in section 4. Conclusions and recommendations for further study are presented in section 5.

2. Background

The northward progression of stratus along the California coast was first documented on satellite images by the National Weather Service (NOAA 1969), but no attempt was made to define or explain the phenomenon. Jackson (1983) observed that the northward movement of stratus frequently appeared when the

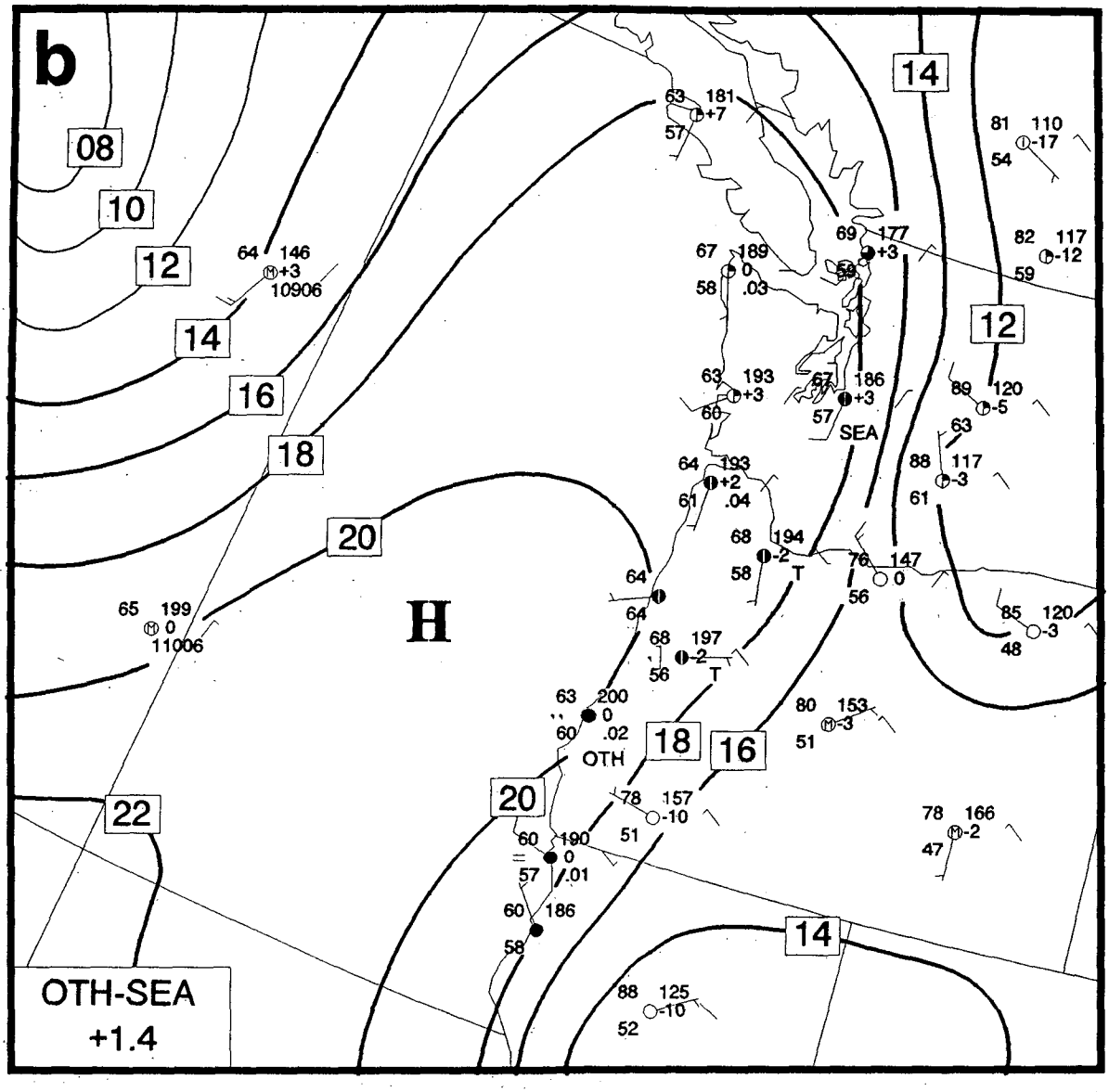

FIG. 5. (*Continued*)

(SSD) for their encouragement in supporting this effort. Tim Barker, also from SSD, provided considerable editing advice and assistance with figures—his expertise is most appreciated.

REFERENCES

Jackson, B., 1983: Dealing with the thermal trough. Western Regional Technical Attachment No. 83-21, 6 pp. [Available from the National Weather Service Western Region, P.O. Box 11188, Salt Lake City, Utah 84147.]

——, 1984: Terminal forecast pitfalls. Western Regional Technical Attachment No. 84-07, 2 pp. [Available from the National Weather Service Western Region, P.O. Box 11188, Salt Lake City, Utah 84147.]

Kinzebach, R. M., 1955: An objective method of forecasting the occurrence of low clouds in the McChord–Seattle area during the summer months. *Bull. Amer. Meteor. Soc.*, **36,** 104–108.

Mass, C., and M. D. Albright, 1987: Coastal southerlies and alongshore surges of the west coast of North America: Evidence of mesoscale topographically trapped response to synoptic forcing. *Mon. Wea. Rev.*, **115,** 1707–1738.

——, ——, and D. J. Brees, 1986: The onshore surge of marine air into the Pacific Northwest: A coastal region of complex terrain. *Mon. Wea. Rev.*, **114,** 2602–2627.

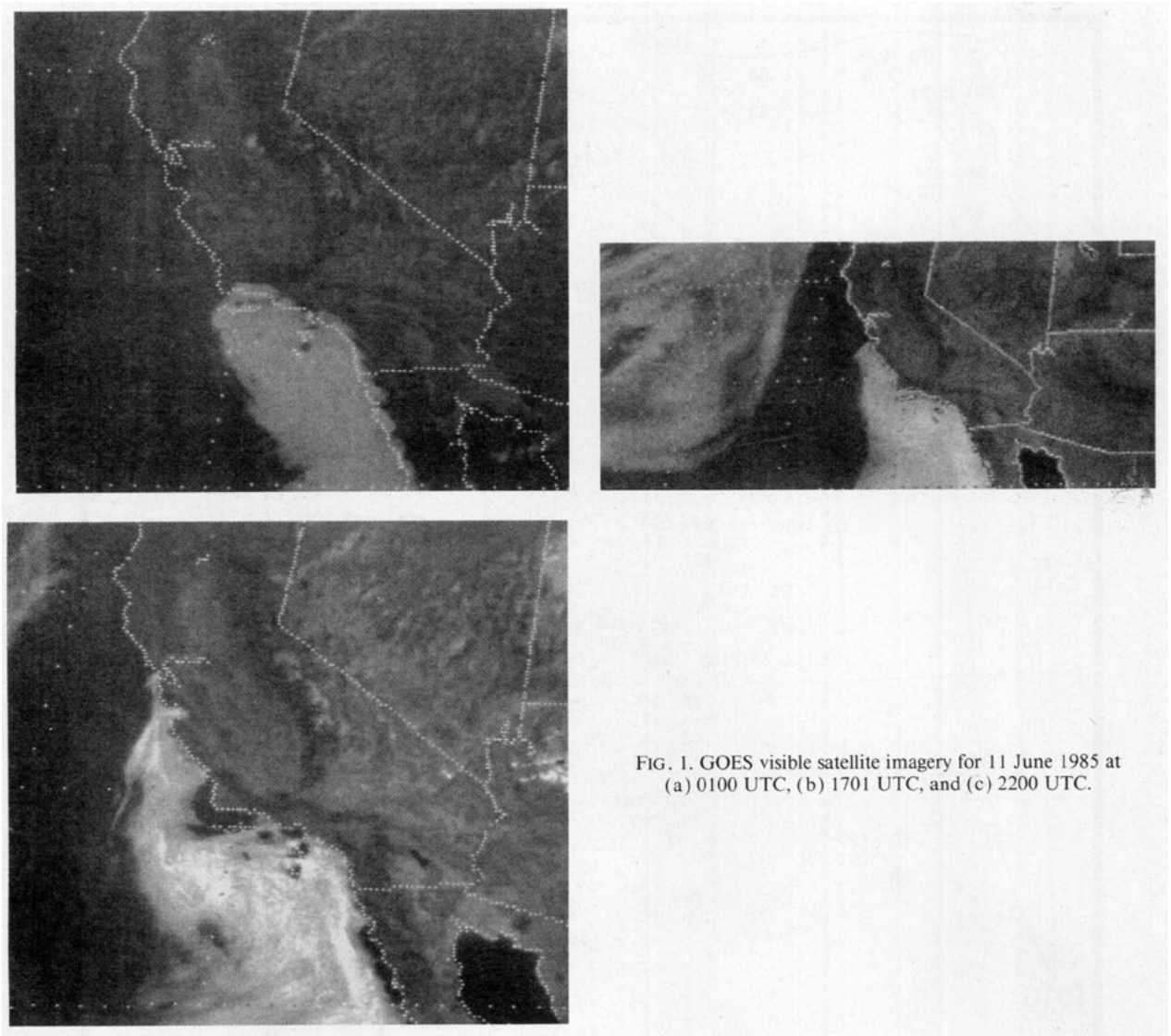

FIG. 1. GOES visible satellite imagery for 11 June 1985 at (a) 0100 UTC, (b) 1701 UTC, and (c) 2200 UTC.

California heat trough extended to the coast, west of its normal inland position (see, also, Gilliland 1980). Dorman (1985) presented a case study of a May 1982 event that progressed from Pt. Conception to Cape Mendocino over a 3-day period and suggested that northward-progressing stratus surges were due to coastally trapped Kelvin waves.

Mass and Albright (1986) analyzed a synoptically forced surge that progressed from central California to Vancouver Island. They hypothesized that an upper-level low circulation over southern California caused the cool marine layer to deepen in the south, reversing the mesoscale pressure gradient along the coastline and triggering the surge event. At low levels, a narrow zone of ageostrophic downgradient flow developed and progressed northward. The width of this zone was limited because geostrophic balance was impeded by the presence of the coastal mountain barrier. Mass and Albright (1986) also reanalyzed the Dorman case study and showed that the Kelvin wave hypothesis was not consistent with observational evidence.

Although the Dorman (1985) and Mass and Albright (1986) studies revealed some very important mechanisms for stratus surge initiation and progression, those studies involved two strong and particularly well-defined cases. In an attempt to generalize their results and apply them to the local forecast problem, an effort is made here to examine a large sample of stratus surges and to characterize them using available meteorological data.

3. Climatological study and conceptual model

In a preliminary investigation, a climatology of stratus surge events along the West Coast of the United States was developed. The climatology was developed on the basis of a study of visible satellite imagery from 23 well-defined stratus surges for the period 1975–1985.

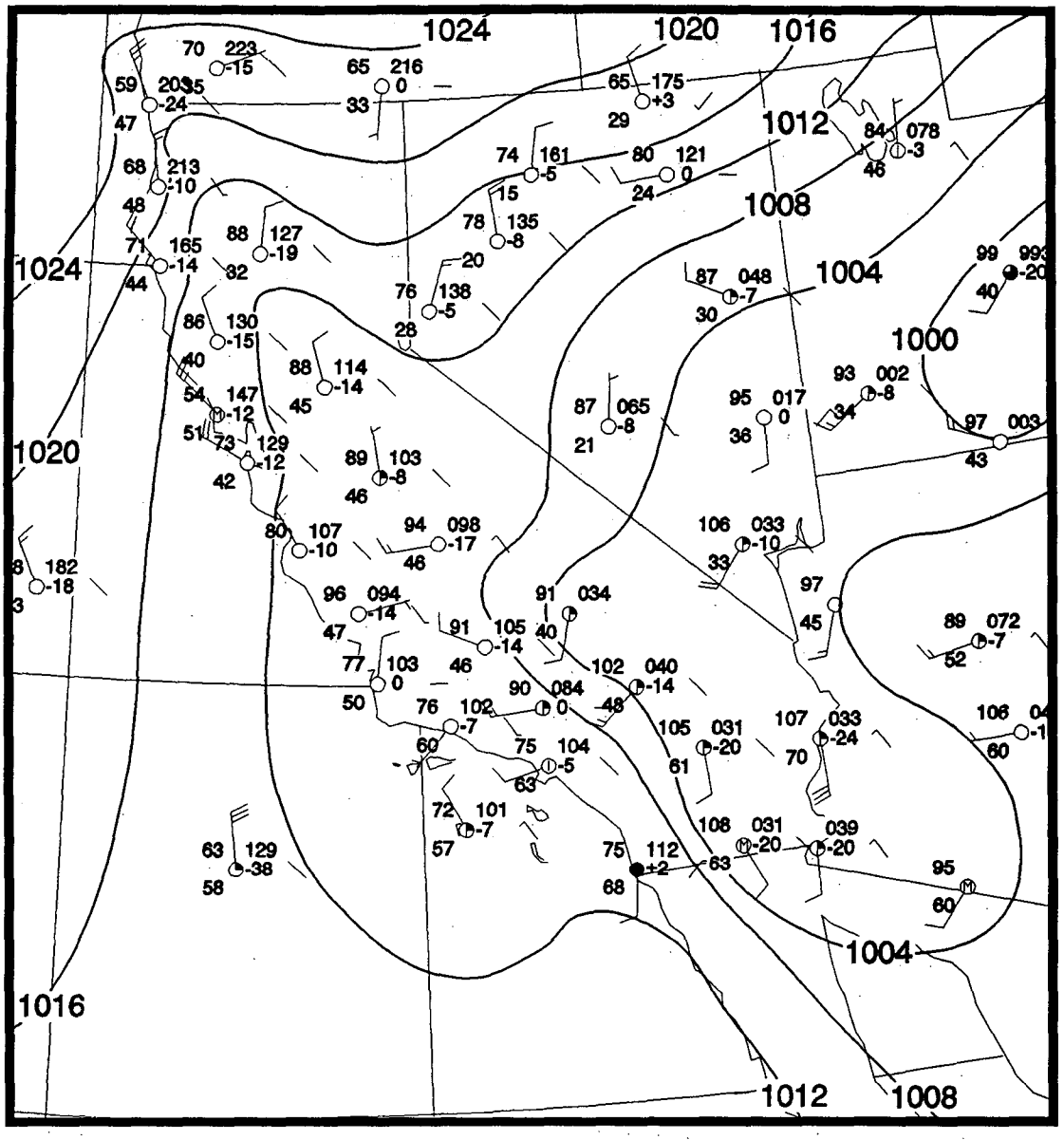

FIG. 2. Surface chart valid at 0000 UTC 8 July 1981 showing the surface heat trough over southern California. Conventional surface station plots with wind speed in knots, temperatures in degrees Fahrenheit, and sea level pressure in tenths of millibars with the first two digits dropped. Isobars at 4-mb intervals.

A *stratus surge* is defined as the northward progression of a narrow band of stratus along the central California coast between Pt. Conception and Pt. Reyes. Surface, 850-mb, and 500-mb charts were examined to establish a composite pattern at surge initiation. The composite patterns produced were averaged from the 23 stratus surge events.

A common surface pressure pattern featured the axis of the California heat trough aligned from the northwest corner of California through the Central Valley, with a very weak extension to this trough evident at the surface along the central California coast (Fig. 2). Two upper-air circulation patterns that could result in these surface features were associated with the development of surge events. One pattern, observed prior to 11 of the 23 events, featured an upper-level low circulation over, or to the south of, the central California coast (Fig. 3). For the remaining cases, the axis of an upper-level short-wavelength ridge was aligned northeast–southwest across northern California. At 850 mb, this synoptic pattern results in ridging over northern California and troughing over the southern coastal area (Fig. 4). Both upper-air patterns can produce low-level offshore flow and a shallow marine layer (low inver-

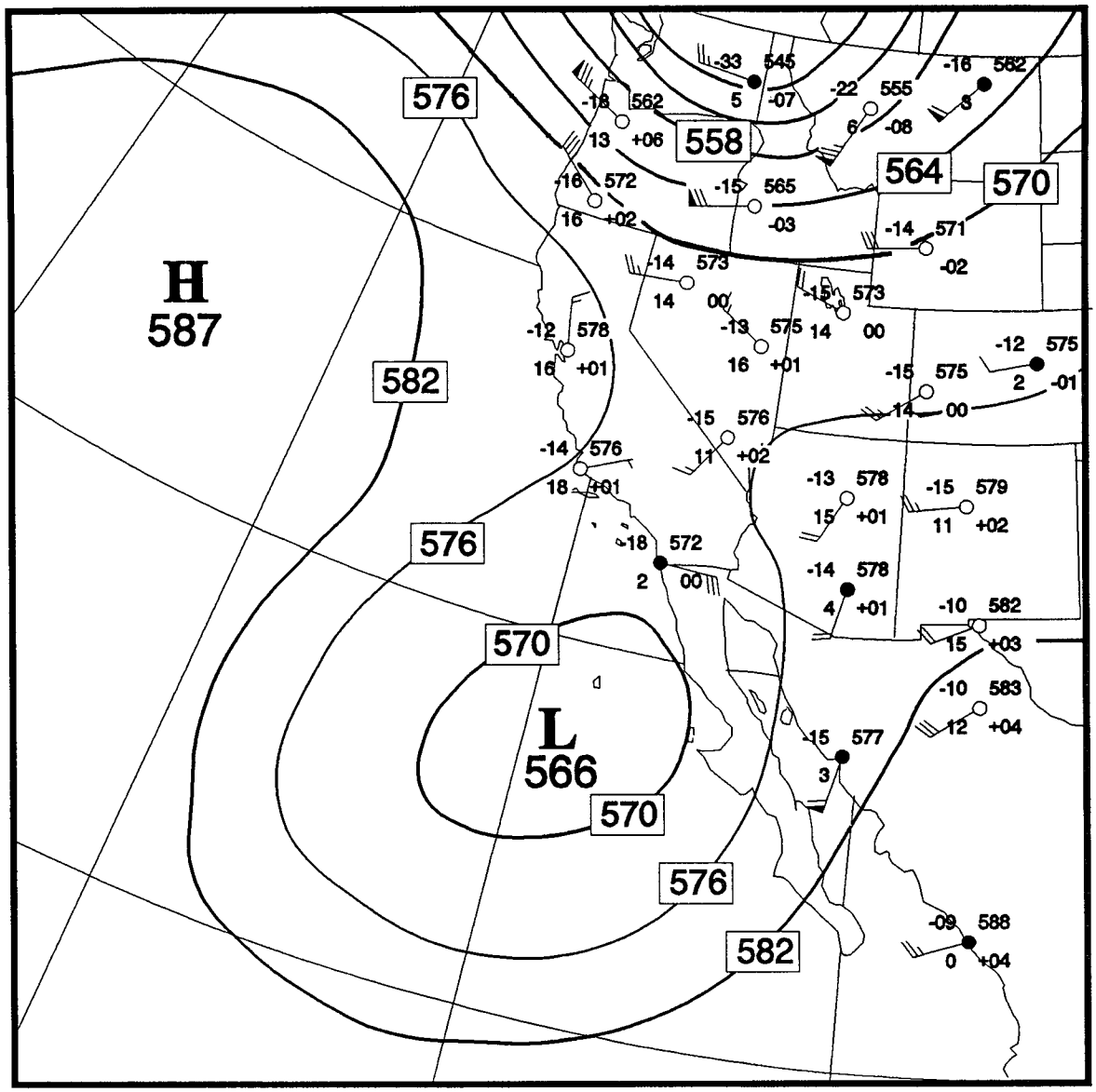

FIG. 3. Here a 500-mb chart valid at 0000 UTC 4 May 1982 showing "cutoff low" pattern associated with the stratus surges. Conventional station plots with wind speed in knots and height in decameters. Height contours at 6-dam intervals.

sion) to the north and a deeper marine layer (higher inversion) to the south. As short-wavelength ridging occurs in the north, the inversion tends to be lowered due to downward vertical motion. The opposite occurs in the south where lower pressure exists and a weaker inversion is elevated due to upward vertical motion. During these conditions, a mesoscale alongshore pressure gradient conducive to localized southerly flow can result.

The aforementioned synoptic composite patterns are summarized as 500-mb map types for the initiation of stratus surge event:

1) Type 1. Short-wavelength ridge axis over the Pacific Northwest with trough in the Southwest (Figs. 2 and 4).

2) Type 2. Closed midtropospheric low (Fig. 3).

A noteworthy observation in the preliminary study was that all surge events identified began during the nighttime hours, that is, after the last available visible satellite image of the day and before the first visible image the next morning. The mesoscale pressure gradient during the nighttime hours is important to the nocturnal initiation of surges. After sunset, radiative cooling of the land reduces the land–sea temperature differential, thereby relaxing the larger-scale pressure gradient. Northwest winds and low-level convergence along the

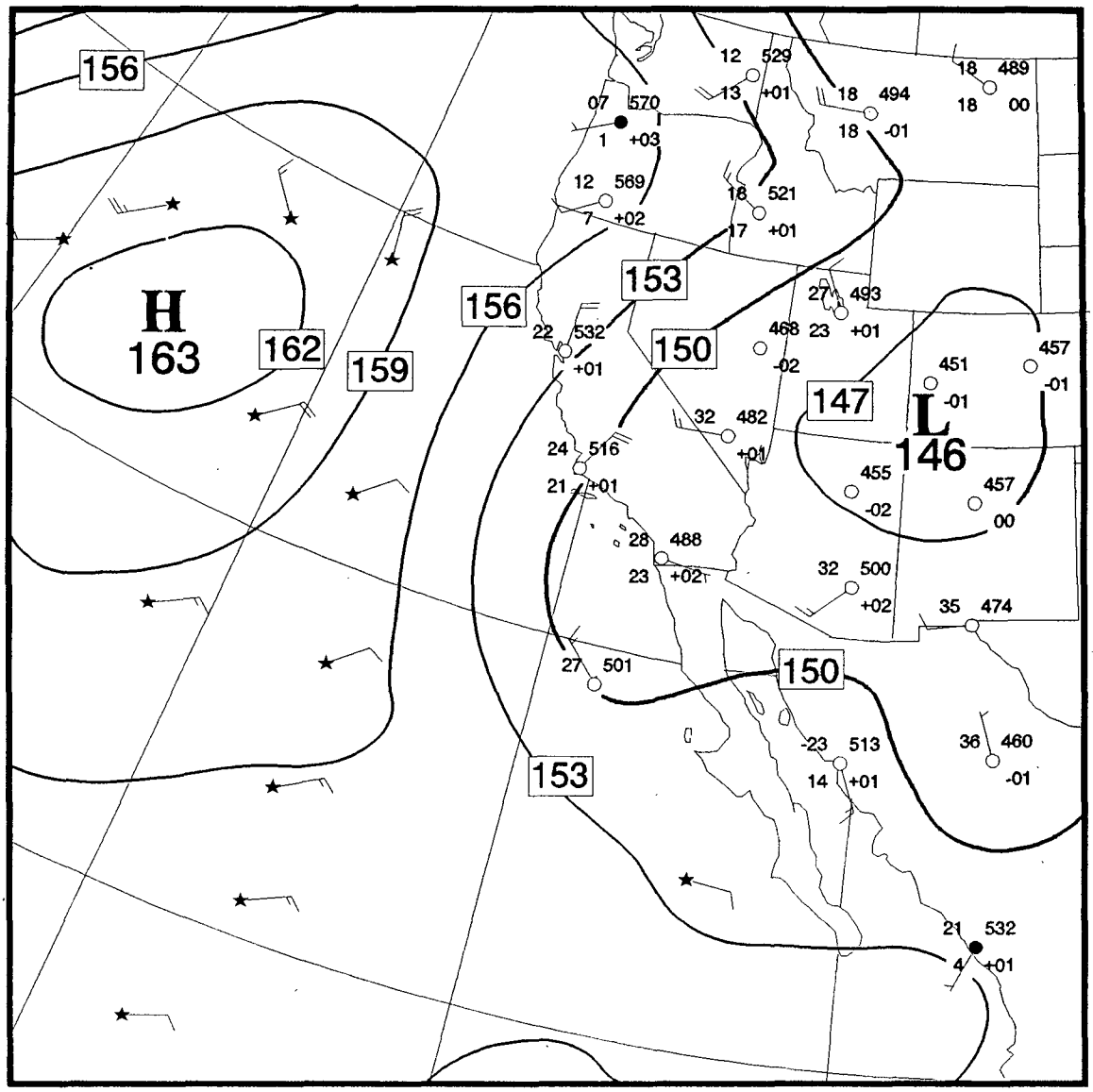

FIG. 4. Here a 850-mb chart valid at 0000 UTC 13 July 1979 showing a typical pattern associated with stratus surges. Conventional station plots with wind speed in knots and height in meters with the first digit dropped. Height contours at 30-m intervals and labeled in decameters.

coast, which are sustained by the synoptic-scale pressure gradient, also subside as the near-surface winds decouple from the boundary layer. A surge can develop when an alongshore mesoscale pressure gradient exists, featuring higher surface pressures to the south. The average surge identified in this study had a life span of 72 h, and event durations ranged from 14 to 144 h. Eleven of the 23 events did not progress north of the California–Oregon border.

Based on this climatology and case study analyses of Dorman (1985) and Mass and Albright (1986), a conceptual model of the stratus surge emerges. Prior to surge development, upper-level ridging exists over northern California. The surface heat trough is displaced coastward from its normal position. This pattern is related to lower than normal sea level pressures, a low inversion, and clear skies along the central California coast. At the same time, the marine inversion in the south has risen, establishing a localized reversal of the normal pressure gradient. During the nighttime hours, the mesoscale pressure gradient becomes more dominant as the larger-scale pressure gradient relaxes. Ageostrophic southerly flow is initiated at the location of the steepest slope of the inversion. The stratus signature of the surge event appears as the inversion rises locally to a height above the lifting condensation level. A similar feature has been studied along the South African coast by Gill (1977).

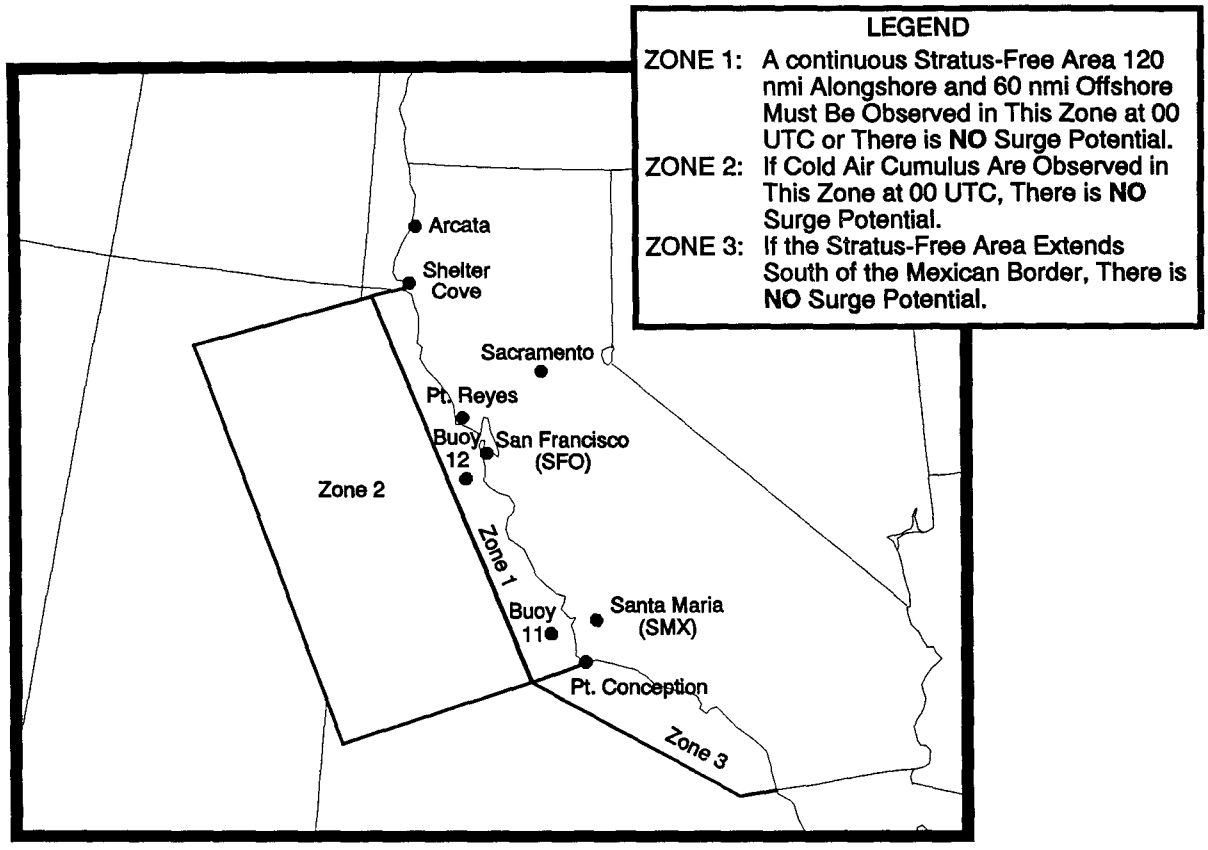

FIG. 5. Criteria and locations used in subjective screening of visible satellite images to determine potential surge events.

4. Forecast model

a. Development

Public, marine, and aviation forecasters face the difficult task of predicting the onset of a stratus surge after one or more days of clear skies along the California coast, and recognizing the synoptic characteristics that may lead to these stratus surges. Drawing on the climatology and the conceptual model described already, a semiobjective forecast technique was developed to predict the initiation of stratus surge events along the central California coastline during the stratus season. The criteria for screening visible-band satellite images to determine potential surge events is shown in Fig. 5. The progression of the stratus surge must be at least 60 n mi (111 km) in the 24-h period after 0000 UTC. "Surge" and "no surge" forecasts are verified using satellite images.

The forecast scheme was developed using the results of an evaluation of satellite images, and surface and upper-air meteorological observations from May through October 1981–1983. The technique is composed of two parts: one subjective and one objective. In the subjective portion, the 0000 UTC (or latest afternoon) visible satellite image is screened to determine if the potential for stratus surge development exists. Once a potential event is identified, the objective part of the scheme evaluates data from the 0000 UTC Oakland sounding and the 0000 UTC sea level pressure distribution along the coast to make a "surge" or "no surge" forecast.

In the subjective screening of satellite images, it was assumed that a surge would not develop if stratus was observed along the entire central California coastline at 0000 UTC. A potential stratus surge was identified if the 0000 UTC satellite image showed a stratus-free zone extending at least 60 n mi (111 km) offshore and 120 n mi (222 km) alongshore south of Shelter Cove (Fig. 5) but not extending south beyond the Mexican border. Furthermore, the stratus-free zone could not be bounded to the west by cold air cumulus clouds within 300 n mi (556 km) of the coast (eliminating strong, postfrontal northwest flow situations). The subjective criteria are described graphically in Fig. 5.

For the 525 days during the model development period that satellite images were available, 170 were classified as "potential" surge days based on a review of the 0000 UTC images. Stratus surges developed in the study area on 41 days (24%). No surges were observed on the days identified as having "no potential." Consistent with the findings of the climatology discussed

earlier, all surge events developed during the nighttime hours.

The objective portion of the forecast technique was developed using predictors that provided some objective description of the marine inversion strength and alongshore sea level pressure field at the beginning of the forecast period. One restriction was that the predictor had to be a routine National Weather Service observation that was generally available for the model development years, and is still part of the current NWS data stream. A preliminary objective forecast scheme was developed using multiple predictors including:

1) 0000 UTC surface pressure readings for Arcata, San Francisco, Santa Maria, Sacramento, buoy 11, and buoy 12;
2) 0000 UTC alongshore and across-shore pressure gradients derived from the foregoing stations; and
3) 0000 UTC Oakland radiosonde mandatory-level temperature, wind, and pressure surface height at three levels (850, 700, and 500 mb).

b. Testing

A forecast model using 10 of the parameters listed in the preceding subsection was developed and tested. This initial modeling effort demonstrated stratus surge forecasting skill, using the skill score method presented in appendix B. However, a model constructed using just two of the most promising predictors [the Santa Maria to San Francisco pressure difference (DPSFSM) and the Oakland 850-mb temperature (T850)] resulted in nearly identical stratus surge forecasting skill. Since the 2-parameter objective model had the same skill as the 10-parameter model, and would be much easier to implement in an operational mode, it was chosen for this application.

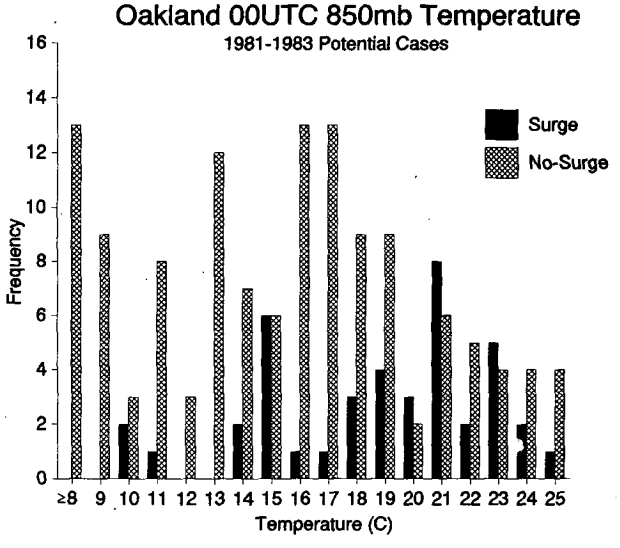

FIG. 6. Frequency distribution (in 1°C bins) of "surge" and "no surge" events as a function of Oakland 850-mb temperature at 0000 UTC. Data from developmental dataset, 1981–1983.

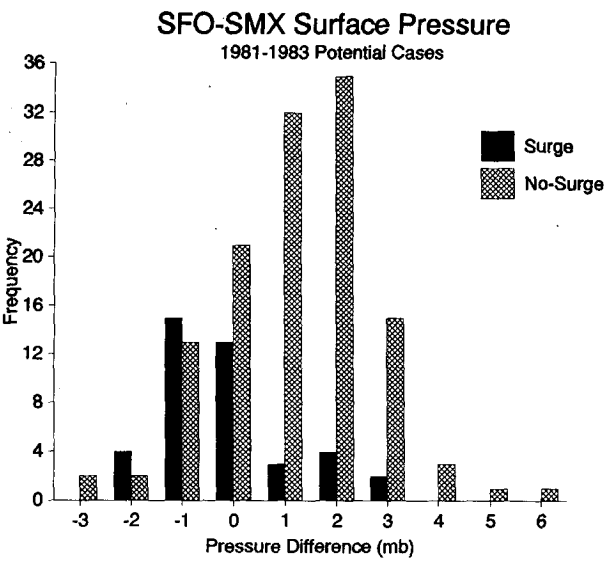

FIG. 7. Frequency distribution (in 1-mb bins) of "surge" and "no surge" events as a function of San Francisco (SFO) to Santa Maria (SMX) pressure difference at 0000 UTC.

Frequency distributions of T850 and DPSFSM for all potential surge days are shown in Figs. 6 and 7. Data for T850 were available for 164 of the 170 potential surge event days. Data for the missing dates were estimated by interpolating between the previous and following 0000 UTC T850s. Data for the 0000 UTC DPSFSM were available for 133 cases. Missing data were estimated statistically using the buoy 11–buoy 12 pressure difference, a process described in appendix A. The T850 histogram shows that surges did not occur at the low end of the temperature range, that is, when the inversion was too high, too weak, or nonexistent. Surge and nonsurge events were fairly evenly distributed at the higher temperatures. The pressure difference histogram presented in Fig. 7 shows a near-normal distribution of surge events. The mode is slightly negative; that is, surface pressures were higher at Santa Maria than San Francisco. For the nonsurge cases, peak frequencies of DPSFSM occurred when the 0000 UTC San Francisco surface pressure was slightly higher than observed at Santa Maria.

Based on the aforementioned frequency distributions, a two-step procedure was developed to objectively forecast surge initiation for the 170 potential cases. The first step consisted of making a "no surge" forecast when the 0000 UTC T850 was below 9.8°C, the level below which no surge events were observed. As a result of this test, 22 of the 170 cases were eliminated as potential events.

The second step of the objective portion of the forecast method consisted of making a "surge" or "no surge" forecast for the remaining potential events based on the value of DPSFSM at 0000 UTC. The pattern

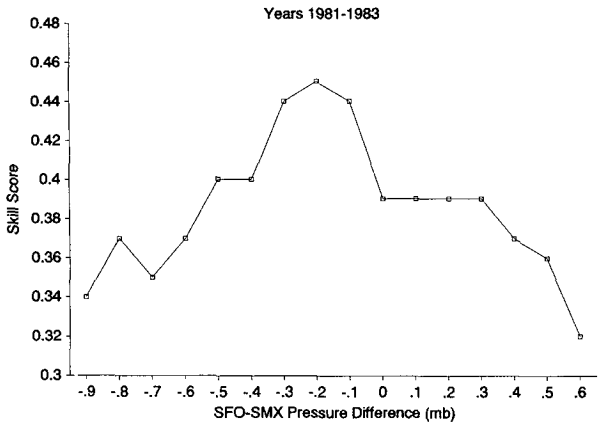

FIG. 8. Skill scores plotted as a function of the threshold value of SFO − SMX pressure difference used to forecast surge development.

shown in Fig. 7 suggests that there was an optimum San Francisco–Santa Maria pressure difference threshold value above which surges were likely to develop and below which surges were unlikely to develop. Skill score calculations, based upon the method described in Panofsky and Brier (1968), were used to determine the optimum threshold value to be used to predict surge development. The method used to calculate skill score is presented in appendix B. Results of the skill score computations, presented in Fig. 8, indicate that forecasting skill was optimized (skill score = 0.45) if surges were forecast when the 0000 UTC DPSFSM was less than or equal to −0.2 mb.

A contingency table showing the results of "surge" and "no surge" forecasts made for the model development dataset using DPSFSM less than or equal to −0.2 mb as the predictor for surge development is presented in Table 1. Over 68% (28 of 41) of the surge events and 79% (85 of 107) of the nonsurge events were correctly forecast. The contingency table also shows that the probability of surge development when "surge" was forecast was 56% (28 of 50). The probability of surge development when a "no surge" forecast was made was 13% (13 of 98). These results indicate that the greatest strength of the objective portion of this forecast scheme is the ability to identify nonsurge events. Very likely this is due to stronger measurable synoptic-scale influences in the nonsurge events and poorly measured mesoscale influences in the surge cases.

TABLE 1. Contingency table of "surge"/"no surge" events for developmental years 1981–1983.

	Forecast		
	"Surge"	"No surge"	
Observed			
"Surge"	28	13	41
"No surge"	22	85	107
	50	98	148

TABLE 2. Contingency table of "surge"/"no surge" events for 1984.

	Forecast		
	"Surge"	"No surge"	
Observed			
"Surge"	20	7	27
"No surge"	7	28	35
	27	35	62

The model was tested using data from the months of May–October 1984. Satellite images were available for 177 days during that period. Using the subjective screening technique, 67 potential surge cases were identified. Satellite images indicated surges developed within 24 h on 27 (40%) of the potential surge days. All surges began during the nighttime hours. In no cases were surges identified within 24 h of 0000 UTC when the subjective screening tests resulted in a "no surge" forecast.

The 67 cases were further screened using the objective portion of the model. Five of the potential cases were eliminated as "no surge" cases on the basis of the T850 criteria. All were correct forecasts. Of the remaining cases, the DPSFSM criteria resulted in 27 "surge" forecasts and 35 "no surge" forecasts. For the test dataset, 74% of the "surge" forecasts and 80% of the "no surge" forecasts verified. Based on the contingency table presented in Table 2, a skill score of 0.54 was attained, somewhat higher than calculated for the development period. Similar to the forecast verification pattern for the development years, the test-year results show that the probability of accurately predicting nonsurge events was higher than for surge events.

A summary of the instructions for implementing the stratus surge forecast model developed here is presented in a flowchart format in Fig. 9. One feature of the model is that the user may exit the model any time a "no surge" forecast is made. In this respect, this semiobjective forecast scheme has many of the characteristics of a decision-tree forecast technique in which a logical series of questions branch out toward the solution of a problem. Ellrod (1989) suggests that the decision-tree approach is well suited for problems involving both subjective and objective criteria.

5. Conclusions and recommendations

It is a difficult task for the local forecaster to predict the onset of stratus after one or more days of offshore flow and clear skies along the West Coast of the United States during the summer season. Very little documentation has been made of the synoptic and mesoscale characteristics of stratus surges along the West Coast. Past case studies of stratus surge events along the California coast by Dorman (1985) and Mass and Albright (1986), and the climatological review, proved

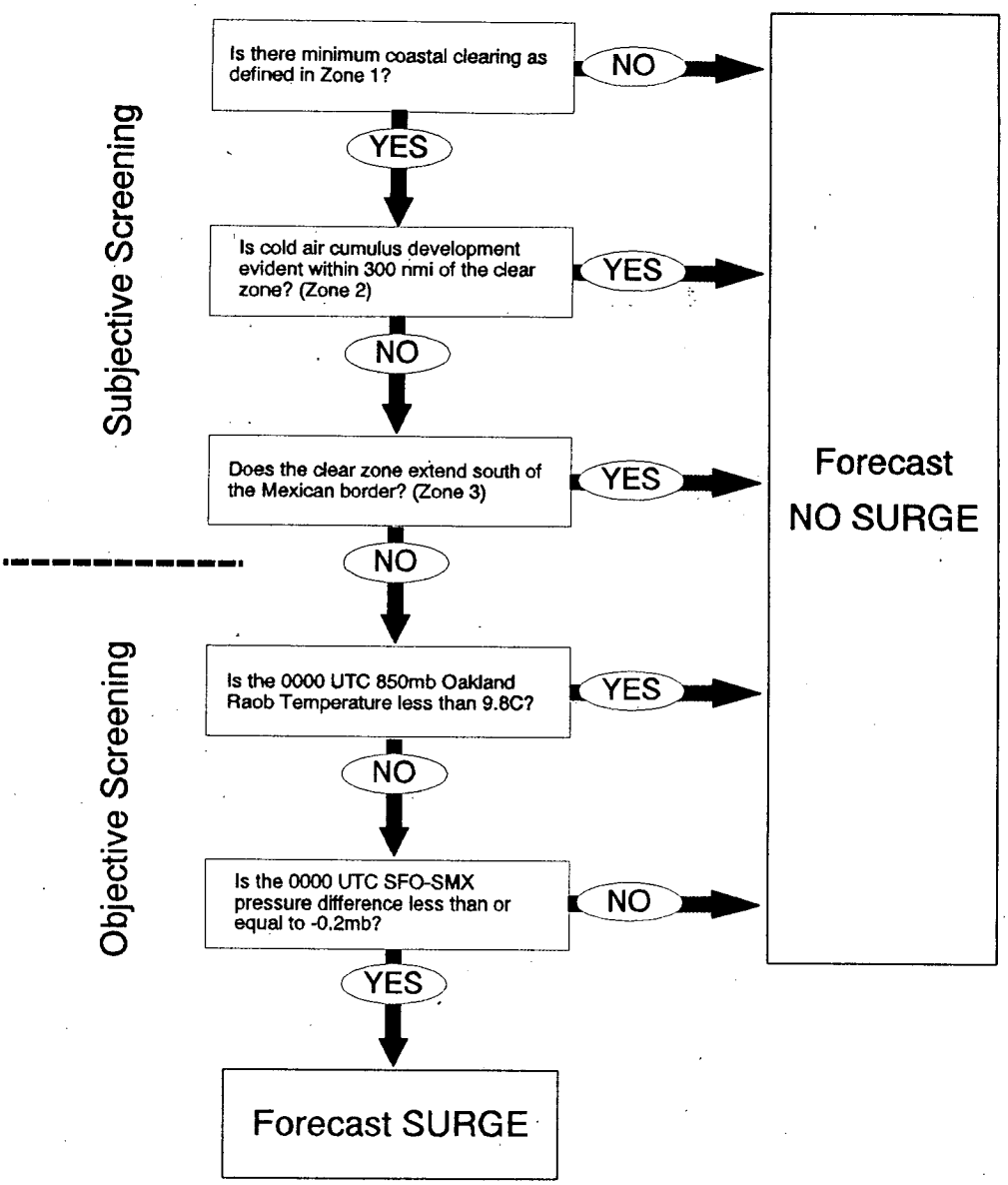

FIG. 9. Stratus surge forecast flowchart.

to be useful tools for developing a method to forecast that phenomenon.

On the synoptic scale, the preliminary climatological study found that prior to surge development, an upper-level short-wavelength ridge exists over northern California, occasionally featuring an upper-level low circulation over, or to the south of, the central California coast. At 850 mb, this synoptic pattern results in ridging over northern California and troughing over the southern coastal area. These upper-air patterns can produce low-level offshore flow and a shallow marine layer (low inversion) to the north, and a deeper marine layer (higher inversion) to the south.

The subjective and objective portions of this model give some indication of both the synoptic-scale and mesoscale atmospheric conditions necessary for stratus surge initiation. In summary, those conditions allow the marine layer to the south to rise (with higher surface pressure) while the marine layer to the north remains shallow (with lower surface pressure), resulting in a weakening or reversal of the normal pressure gradient. The development of surges was consistently observed during the nighttime hours when the synoptic-scale northwest gradient weakens or reverses due to radiative cooling of the land, increasing the importance of the alongshore mesoscale gradient, with higher surface pressure values developing to the south. A majority of surges were observed when the surface pressure was higher at Santa Maria than San Francisco at 0000 UTC, but a reversal of this pressure gradient was not a necessary condition for surge development. Since these stations are approximately 175 n mi (323 km) apart,

it is probable that the spatial scale used to define the pressure gradient in the model is too large to identify some mesoscale events. This semi-objective forecast technique verified well using an independent dataset. It provides the forecaster with a simple and easy-to-implement prediction method, and offers some guidance to the future development of better techniques.

Alongshore pressure tendency and/or pressure gradient tendency, not evaluated in this forecast scheme, may provide additional skill in forecasting surges if included in the objective screening step. It may also be possible to improve forecast skill by including computer model 12- or 24-h forecasts of surface pressure patterns. Model output 500-mb vorticity advection patterns may also have predictor value for forecasting the marine-layer depth, in response to changes in upper-level dynamics.

No attempt was made to forecast the northward extent of the stratus surge or predict the duration of events, which may be as important as forecasting the event itself. This deserves further study. Also, eddies have been observed to form at the leading edge of a stratus surge when it encounters coastal headlands. Further study of this phenomenon may lead to a better understanding of the stratus surge life cycle and the effect that topographic features along the coast have on surge duration.

Operationally, both National Weather Service offices in Redwood City and Santa Maria have used the stratus surge prediction scheme with some success. The two offices have coordinated and discussed potential surge events looking at the prediction scheme in real time over the last two years. However, the frequency of stratus surge events the last two years has been low, and more recent objective scorings have not been attempted.

Acknowledgments. The authors wish to acknowledge Dr. Peter Lester at San Jose State University and Tim Barker at Western Region Headquarters, National Weather Service, for their help and encouragement in this research.

APPENDIX A

Estimating San Francisco–Santa Maria Pressure Gradient

Although DPSFSM data were available for most of the model development and test years, there were some missing data. To evaluate this parameter for all potential surge days identified in the subjective portion of the model, a method was developed to estimate DPSFSM based on the pressure gradient between buoy 12 and buoy 11 (DP1211). These buoys are located approximately 30 miles (55 km) offshore near the northern and southern boundaries of the study area (Fig. 5). Buoy 11 is located directly west of Santa Maria, and buoy 12 is located about 20 miles (37 km) south-southwest of San Francisco International Airport. Available 0000 UTC pressure gradient data from both sources (sample size = 285) were statistically analyzed using a general linear models procedure (SAS 1985). A good correlation was found between DPSFSM and DP1211 ($R^2 = 0.75$), and the equation to estimate the 0000 UTC DPSFSM using the observed 0000 UTC DP1211 and the slope and intercept output by the general linear model was

$$\text{DPSFS} = (\text{DP1211} \times 0.7807) - 0.943.$$

This equation was used to estimate missing alongshore pressure differences.

APPENDIX B

Skill Scores

Skill scores (S) were are defined as $S = (R - E)/(T - E)$, where R is the number of correct forecasts, T is the total number of forecasts, and E is the number of forecasts expected to be correct (Panofsky and Brier 1968). Here S has a value of zero if the number of correct forecasts equals the number of expected correct forecasts, and approaches unity as forecast skill increases. In a purely chance forecast situation, such as a coin flip, the value of E is one-half of T. Since surge events were observed only on about one-fourth of the potential surge days, E was calculated using the margin totals of the contingency tables as suggested by Panofsky and Brier (1968). The expected number of correct forecasts was therefore calculated using

$$E = R_i \times C_i / T,$$

where R_i is the sum of the ith row and C_i is the sum of the ith column.

REFERENCES

Dorman, C. E., 1985: Evidence of Kelvin waves in California's marine layer and related eddy generation. *Mon. Wea. Rev.*, **113,** 827–839.

Ellrod, G., 1989: A decision tree approach to clear air turbulence analysis using satellite and upper air data. NOAA Tech. Memo. NESDIS 23, NOAA/NESDIS, 20 pp. [Available from World Weather Building, Washington, DC 20233.]

Gill, A. E., 1977: Coastally trapped waves in the atmosphere. *Quart. J. Roy. Meteor. Soc.*, **103,** 431–440.

Gilliland, R. P., 1980: The structure and development of the California heat trough. M. S. thesis, Department of Meteorology, San Jose State University, 90 pp.

Jackson, B., 1983: Dealing with the thermal trough. Western Regional Tech. Attachment No. 83-21, 6 pp. [Available from the National Weather Service Western Region, P.O. Box 11188, Salt Lake City, UT 84147.]

Mass, C. F., and M. D. Albright, 1986: Coastal southerlies and alongshore surges of the west coast of North America: Evidence of mesoscale topographically trapped response to topographic forcing. *Mon. Wea. Rev.*, **115,** 1707–1738.

Panofsky, H. A., and G. W. Brier, 1968: *Some Applications of Statistics to Meteorology.* Pennsylvania State University Press, 222 pp.

1985: *SAS Users Guide: Statistics.* Version 5. SAS Institute Inc., 1290 pp.

NOAA, 1969: Stratus plume details by satellite. Western Region Tech. Attachment No. 69-24, 2 pp. [Available from the National Weather Service Western Region, P.O. Box 11188, Salt Lake City, UT 84147.]